

Simulation of a spray scrubber performance with Eulerian/Lagrangian approach in the aerosol removing process

Y. Bozorgi, P. Keshavarz, M. Taheri, J. Fathikaljahi*

Department of Chemical and Petroleum Engineering, College of Engineering, Shiraz University, Shiraz, Iran

Received 27 July 2005; received in revised form 23 January 2006; accepted 20 February 2006

Available online 4 April 2006

Abstract

In this study, a mathematical model has been developed to simulate the performance of a spray scrubber in an industrial ammonium nitrate plant. The model is based on the Lagrangian approach for the droplets movement and particle source in cell (PSI-CELL) model for calculating the droplet concentration distribution. Consequently, unlike former research, the emphasis is on the droplet dynamic behavior. In the current study, for approaching a realistic model, a droplet size distribution rather than average diameter, and also liquid film formation rather than uniform and constant droplet flow rate has been applied. Also, the Eulerian method has been used for the calculation of the particles removal efficiency and energy balance has been applied on the gas to estimate the droplet size distribution. In the experimental section, the concentration of particles and their size distribution in both inlet and outlet gas of the studied scrubber has been measured for the validation of the predicted particles collection efficiency. In addition, the temperature of the gas at inlet, outlet and in the middle of the tower has been measured for the confirmation of the predicted droplet size distribution in the tower. A good consistency between the model and data has been observed. After the model is validated, it is used to investigate the various variable profiles such as liquid film, total projected surface area of the droplets, velocity profile of the droplets and some of the other parameters in the spray scrubbers.

© 2006 Elsevier B.V. All rights reserved.

Keywords: Spray scrubber; Lagrangian; Eulerian; Collection efficiency

1. Introduction

One of the classical types of air pollution control equipment is spray scrubber, which have been used for many years in industry. A simple design, low pressure drop and low maintenance costs are its advantages, while the high consumption of liquid and lower efficiency in comparison with other scrubber types in gas scrubbing and particle removing are the disadvantages of this equipment.

Several attempts have been made to investigate the performance of this kind of system. The first elaborate study about the spray type of towers was presented by Pigford and Pyle [1], in which the gas scrubbing process was experimentally investigated. They also did experiments on the effect of many parameters like liquid to gas ratio, droplet size distribution, nozzle type, liquid film formation and various design parameters

on the tower performance. Their study was of a more experimental basis rather than a theoretical one. Sharma and Mehta [2] explored the gas mass transfer operation in spray towers. In their research, liquid film formation has been overlooked, although they have pointed out that such a liquid film does exist, and is not ignorable. Hollands [3] investigated a cooling spray tower performance with no liquid film consideration. Michalski [4] probed the dynamic behavior of the liquid droplets; but in his mathematical model for the droplets movement, the droplets motion were regarded as one dimensional in the tower height direction (naturally, unable to predict the liquid film formation). Brogen and Karlsson [5] simulated the absorption of SO₂ by liquid lime by using the penetration theory, but their study was of a case study of mass transfer operation rather than a spray scrubber performance investigation. Like their previous colleagues, they had used an average diameter rather than droplets size distribution. Makkinejad [6] shows the effects of various parameters on the temperature profile of both closed and open loop spray towers. Rahimi et al. [7] expanded momentum, mass, and especially, energy balances for the droplets in two small case studies of hot

* Corresponding author. Tel.: +98 711 2303074; fax: +98 711 6287294.
E-mail address: zeglda@shirazu.ac.ir (J. Fathikaljahi).

Nomenclature

$A(\theta_i)$	total area covered by the flow rate, $Q(\theta_i)$
B	$C_{pv}\Delta T/\Delta H_v$
$C_{D,i}$	drag coefficient corresponding to the i th size of droplets
$C_P(j, z)$	particulate concentration of the j th size of particles in the z th increment of the tower (kg/m^3)
C_{pv}	water vapor heat capacity ($\text{J}/\text{kg C}$)
D_i	diameter of the i th size of droplets (m)
D_{ii}	initial diameter of the i th size of droplets (m)
D_d	droplet diameter (m)
D_G	mass median diameter (m)
f	correction factor for non-uniform distribution movement of the droplets
g	gravity (m/s^2)
G	gas flow rate per unit area ($\text{kg}/\text{m}^2 \text{ s}$)
h	height (m)
$h(i, z)$	heat transfer coefficient corresponding to i th size of droplets at the z th increment of the tower ($\text{W}/\text{m}^2 \text{ K}$)
ΔH_v	heat of vaporization (J/kg)
K	a constant (m/s)
L	length (m)
M	a parameter in energy balance
N	a parameter in energy balance
NO	cumulative fraction for the droplets less than size D_d
Nu	Nusslet number
$\text{Num}(i, z)$	number flow rate corresponding to the i th size of droplets at the z th increment of the tower (number/s)
$\text{Num}(0)$	total number flow rate of the droplets at the starting location (number/s)
Pr	Prantle number
$Q(i, z)$	volume flow rate corresponding to the i th size of droplets at the z th increment of the tower (m^3/s)
Q_g	gas flow rate (m^3/s)
Q_l	flow rate of liquid from each pressure nozzle (m^3/s)
r	radial direction (m)
R	radius (m)
Re_i	Reynolds number corresponding to the i th size of droplets
$Re(i, z)$	Reynolds number corresponding to the i th size of droplets at the z th increment of the tower
t	time (s)
T_g	gas temperature (K)
T_{Di}	droplet temperature corresponding to the i th droplet size (K)
ΔT	$(T_g - T_{Di})$ (K)
v_g	gas velocity (m/s)

$v_r(i, z)$	velocity in r direction corresponding to i th droplets size at the z th increment of the tower (m/s)
$v_\theta(i, z)$	velocity in θ direction corresponding to i th droplets size at the z th increment of the tower (m/s)
$v_z(i, z)$	velocity in z direction corresponding to i th droplets size at the z th increment of the tower (m/s)
$v_e(i, z)$	equivalent velocity corresponding to i th droplets size at the z th increment of the tower (m/s)
x_i	number fraction of the i th droplet size
z	z th increment of the tower
z_{\max}	last increment

Greek symbols

δ	mass standard distribution
η	collection efficiency
η_{overall}	overall collection efficiency
μ	viscosity ($\text{kg}/\text{m s}$)
ρ_L	liquid density (kg/m^3)
ρ_g	gas density (kg/m^3)

Subscripts

i	index for the droplets
j	index for the particles

gas spray cooling towers in two cement plants. Their studies emphasize the simultaneous phenomenon of droplet-gas mass transfer and heat transfer, not the particle removing process. No particle removal studies have been made in their research.

Several attempts have been made to investigate the gas-droplet mass transfer and temperature profile in spray scrubbers [1–8]; however the performance of a spray scrubber for the particle removing process has not been emphasized in previous studies. Even in past studies about gas-droplet mass transfer, the liquid film formation has been overlooked and no attention has been paid to the dynamic behavior of the droplets. These defects have been shed in the current study, and a mathematical model has been developed for the flow which has been discharged from the classical pressure nozzles. The current results can be fruitful in the design and simulation of any spray system.

In the present study, a mathematical model in a cylindrical coordinate has been developed to predict the particle collection efficiencies in a gas stream from a spray scrubber. The current model takes into account the Eulerian approach for the particles dispersion, the Lagrangian approach for the droplets movement, and simultaneously, particle source in cell (PSI-CELL) model to obtain the droplets concentration distribution. It is evident that the gas temperature profile in a spray scrubber or a cooling tower originates from the cooling effects of a definite droplet size distribution. Consequently, energy balance based on a definite droplet size distribution has been applied to the gas in order

to calculate the gas temperature profile. Therefore, for the validation of the obtained gas temperature profile, as well as the consequent validation of the speculated droplet size distribution, temperatures of gas at three different locations of the studied tower have been measured. Besides, for the validation of the predicted particle collection efficiencies, particle concentration and size distribution have been measured in both inlet and outlet gas.

2. The case study specifications and the experimental data

The studied spray scrubber is located in the Shiraz Petrochemical Complex in the ammonium nitrate unit. A schematic of the tower is shown in Fig. 1.

The tower height is 15 m and includes three sections. The first section has a height of about 5 m with a 3.18 m diameter. Each of the second and the third segment heights are 5 m with diameters of 2.1 and 1.7 m, respectively. The nozzles rows are located in the first section of the tower with a 2.2 m distance from each other and situated on the wall of the tower. Each row includes of 10 patent pressure nozzles. In the second and third part of the tower, some patented vanes and gas diverters cause a rotary motion for the gas in these sections. Also a patented cyclonic mist eliminator exists in the second section for capturing droplets. The nozzle fluid discharge velocity is 15 m/s. Table 1 includes the process specifications of the tower.

Experiments and data consist of three sections. The ammonium nitrate particle concentration and also its size distribution are measured by bag filters and Anderson Cascade, respectively, at both inlet and outlet gas. Also, the gas temperature at inlet, outlet and in the middle of the tower has been measured by a

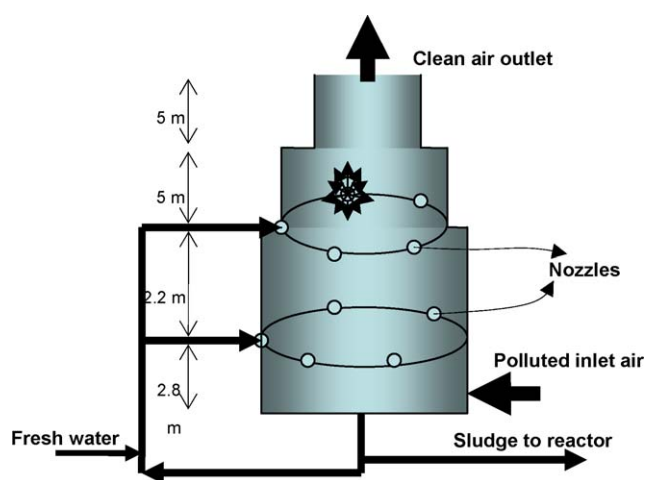


Fig. 1. Schematic of studied tower (scale not observed).

Table 1
Process specifications of the tower

Velocity of gas in the first section (m/s)	4.627
Circulated water flow rate (m ³ /h)	420
Make up flow rate (m ³ /h)	4
Water concentration of sludge (%)	50
Polluted air flow rate (m ³ /h)	130000

Table 2
Mass concentration of ammonium nitrate in inlet and outlet gas of the Scrubber

Stream	(mg particle/m ³ of gas)
Polluted air	14892
Clean air	31.938

Table 3
Mass particle concentration distribution for each particle size in the inlet and outlet air from the studied scrubber

Index	Size distribution (μm)	Particle mass concentration per unit air inlet volume (mg/m ³) in each cut	Particle mass concentration per unit air outlet volume (mg/m ³) in each cut
1	9.85 and more	9681.587	Approximately 0
2	5.2–9.85	4644.666	Approximately 0
3	4.6–5.2	244.229	Approximately 0
4	2.95–4.6	176.619	Approximately 0
5	1.52–2.95	67.312	1.519
6	1–1.52	47.803	9.447
7	0.5–1	19.955	11.352
8	0.24–0.5	9.829	9.621

Table 4
Temperature at three different points of the studied scrubber

Location	Temperature (°C)
Top	37
Bottom	60
First row of nozzles (from the bottom)	43.5

temperature bulb. In order to remove the droplets from the temperature measuring system and prevent the temperature bulb from being affected by the droplets wet bulb temperature, the bulb has been inserted in the outlet gas stream from a small cyclone.

In all these experiments, the velocity of air in the measuring systems is equal to the velocity of the air in the tower (isokinetic condition [9]) in order to minimize errors, especially in the measuring of the concentration and also the particle size distribution.

Table 2 includes the ammonium nitrate concentration in both the inlet and outlet air. In Table 3, particle size distribution in terms of mass (mg/m³) in 8 cut are shown. Temperatures at three different points of the tower are also included in Table 4.

3. Mathematical modeling

The Lagrangian method, which is based on tracking each individual droplet, has been applied for the droplets momentum equations. Also the PSI-CELL model, which is based on the simple system of counting, has been applied for the droplets concentration calculations. In the Eulerian approach, the continuity equation of particles is solved in order to obtain the particles collection efficiencies.

In this study, like previous studies about spray scrubbers, a plug or uniform motion of the gas has been considered. It is

necessary to indicate that for a typical particle size of 10 μm , when subjected to a gas velocity of 4.5 m/s (approximate velocity of the gas in the studied scrubber), the drag force by the gas is more than 300 times greater than the particle gravity force. So certainly the gas carries the particles. This fact justifies the assumption of no relative velocity between the gas and the particles.

The flow from the classical pressure nozzles is usually in cone form [10]. In order to apply the Lagrangian method, and the consequent pursuing of the elements of the fluid which have been discharged from the nozzles, a mathematical model should be derived for this cone. This mathematical model will be presented later.

4. Particulate concentration distribution

For particle loading in a spray scrubber, the continuity equation for each particle cut size can be represented as:

$$Q_g C_p(j, z + dz) - Q_g C_p(j, z) = \sum_{D_{i \min}}^{D_{i \max}} \eta \left(\frac{Q(i, z)}{\pi D_i^3 / 6} \right) \left(\frac{\pi D_i^2}{4} \right) \times (\vec{v}_g - \vec{v}_e(i, z)) C_p(j, z) \frac{dz}{v_z(i, z)} \quad (1)$$

This can be written as:

$$\int d(C_p(j, z) Q_g) = \int_0^L \sum_{D_{i \min}}^{D_{i \max}} \eta \frac{3(Q(i, z))}{2D_i v_z(i, z)} (\vec{v}_g - \vec{v}_e(i, z)) \times C_p(j, z) dz \quad (2)$$

This continuity equation (see nomenclature) can be obtained by the implementation of a mass balance for particulate matter over a cylindrical volume element.

In computing Eq. (2) for predicting particles collection efficiency, one must obtain expressions for the different droplets sizes equivalent velocity at any increment of the tower ($v_e(i, z)$), their z direction velocity ($v_z(i, z)$) and number flow rate ($Q(i, z)/(\pi D_i^3/6)$). In addition, the droplet size distribution and the target efficiency (η) are needed. These variables are discussed in the following sections. Equations of the particle removing process and their essence can be found in many references like Crawford [9].

5. Liquid droplet velocity

When the droplets are dispersed in the tower space, their velocity in all three coordinates of r , z and θ is changing with time (negative accelerating droplets). It is evident that:

$$\frac{dv_z}{dt} = \frac{dv_z}{dz} v_z \quad (3)$$

$$\frac{dv_r}{dt} = \frac{dv_r}{dz} v_z \quad (4)$$

$$\frac{dv_\theta}{dt} = \frac{dv_\theta}{dz} v_z \quad (5)$$

By applying the momentum balance for the droplets in r , z and θ directions and substituting of the above equations in the momentum equations:

$$\frac{dv_z}{dz} = \frac{g(\rho_L - \rho_g)}{\rho_L \vec{v}_z} + \frac{3C_D \rho_g |v_e| (v_g - \vec{v}_z)}{4D_i \vec{v}_z \rho_L} \quad (6)$$

$$\frac{dv_r}{dz} = \frac{|\vec{v}_\theta|^2}{r \vec{v}_z} + \frac{3C_D \rho_g |v_e| \vec{v}_r}{4D_i \vec{v}_z \rho_L} \quad (7)$$

$$\frac{dv_\theta}{dz} = \frac{3C_D \rho_g |\vec{v}_e| \vec{v}_\theta}{4D_i \vec{v}_z \rho_L} \quad (8)$$

According to Calvert [11]:

$$C_{D,i} = \frac{55}{Re_i} \quad (9)$$

The droplet Reynolds number Re_d is:

$$Re_i = \frac{\rho_g |\vec{v}_g - \vec{v}_e| D_i}{\mu} \quad (10)$$

In Eqs. (6)–(8), it is assumed that the probable turbulence or eddies will not influence the droplets dynamic equations. According to Mohebbi et al. [12,13] in the simulation of an orifice scrubber, turbulence is an ignorable parameter on the droplets governing equations because under extreme conditions, the inertia of droplets is about 300 times higher than that of a particle. According to them, this reality justifies ignoring the eddy effects on the droplets dispersion. In spray scrubbers, the droplets are generated by the nozzles and not by the gas. In addition, the gas velocity is much lower in comparison with the orifice types. So the droplets are much coarser than that of orifice types (one can compare the predicted droplet size distribution in this scrubber with the experiments conducted Azzopardi and coworkers [14] in a venturi scrubber). This fact justifies ignoring the effects of probable eddies on the droplets momentum equations in the spray scrubbers.

6. Droplets number flow rate and concentration

The Lagrangian approach based on PSI-CELL model is utilized for obtaining the number flow rate of any droplets size at any section of the tower. The number flow rate of spherical droplets at starting location i is given as:

$$\text{Num}(i, 0) = x_i \text{Num}(0) \quad (11)$$

$\text{Num}(0)$ is the total number flow rate of the droplets at the starting location, and x_i is the number fraction of the i th droplets size. Therefore:

$$\text{Num}(i, z) = \frac{Q(i, z)}{\pi D_i^3 / 6} \quad (\text{See Eq.(1)}) \quad (12)$$

So, the number of droplets at any segment of the tower is calculated by this simple method. Details of this method are given elsewhere [15].

7. Droplet size distribution

According to Masters [10], the square root normal distribution can be used to represent the droplet size distribution:

$$\frac{d(NO)}{dD_d} = \frac{1}{2\sqrt{2\pi D_d \delta_G}} \exp - \left[\frac{(\sqrt{D_d} - \sqrt{D_G})^2}{2\delta_G} \right] \quad (13)$$

It is evident that the cooling process of a gas by the droplets is dependent on the droplet size distribution [6,7], i.e. different droplet size distributions generate different gas temperature profiles. In this study, the equations given by Rahimi et al. [7] have been used to estimate the gas temperature profile in order to validate the speculated droplet size distribution (δ_G and D_G in Eq. (13)) in the tower:

$$\frac{dT_g(z)}{dz} = - \sum_{i=1}^N \frac{6Q(i, z)h(i, z)D_i^2(T_g(z) - T_{Di})}{GC_{pg}D_{ii}^3v_e(i, z)} \times \left[1 + \frac{C_p}{\Delta H_v}(T_g(z) - T_{Di}) \right] \quad (14)$$

In Eq. (14), $h(i, z)$ or heat transfer coefficient corresponding to the i th size of droplets at z th increment of the tower is given by:

$$M = 1 - 0.4 \left(1 - \frac{T_{Di}(z)}{T_g(z)} \right) \quad (15)$$

$$N = 1 - 0.4 \left(1 - \frac{1}{B}(\ln(1 + B)) \right) \quad (16)$$

Then

$$Nu = MN \left(\frac{1}{B} \right) \ln(1 + B)(2 + 0.6Re^{0.5}Pr^{0.3}) \quad (17)$$

In this research, the droplets probable diameter change due to evaporation has been ignored ($D_i = D_{ii}$). As the water injection system is a closed loop type, the temperature of water droplets (T_{Di}) is constant.

8. Target efficiency and overall collection efficiency

Target efficiency (η) in Eq. (1) consists of three coordinates: inertial impaction, interception and diffusion. As their corresponding equations are too long and messy, they are not presented here. The details of these equations are given elsewhere [9].

Generally, the overall collection efficiency is the ratio of the net amount of particles captured to the total amount of input. Therefore, in this study:

$$\eta_{Overall} = 1 - \frac{\sum_{j=1}^8 \int_0^R rv_g C_P(j, z_{max}) dr}{\sum_{j=1}^8 \int_0^R rv_g C_P(j, 0) dr} \quad (18)$$

9. Mathematical model of the cone

In geometry, cone is modeled in spherical coordinate; with three specifications of α, θ and also z (Fig. 2). Any element (not a single point) of the cone is specified by two angles α and also θ .

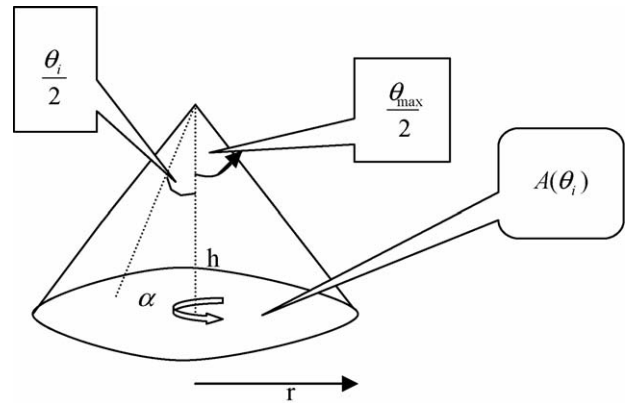


Fig. 2. A cone or schematic of flow from a pressure nozzle.

By the assumption of uniform concentration distribution for the droplets on an imaginary surface below a pressure nozzle, the volumetric flow rate from any height below the nozzle is given by:

$$Q_i(\theta_i) = K \times A(\theta_i), \quad 0 \leq \theta_i \leq \theta_{max} \quad (19)$$

where $A(\theta_i)$ is the total area blotted out by the flow rate $Q(\theta_i)$ on this imaginary surface and K is just a constant which depends on the nozzle type and also distance from the nozzle (later it will be removed from the equations). So, the above equation can be changed into:

$$Q_i(\theta_i) = K \times \pi r^2(\theta_i) \quad (20)$$

As h is the distance of the nozzle from the imaginary surface or $A(\theta_i)$:

$$\tan \left(\frac{\theta_i}{2} \right) = \frac{r}{h} \quad (21)$$

Consequently, by combination of Eq. (20) with Eq. (21):

$$Q_i(\theta_i) = \pi h^2 K \tan^2 \left(\frac{\theta_i}{2} \right) \quad (22)$$

According to the definition of a derivative, the derivative of $Q_i(\theta_i)$ is:

$$Q'_i(\theta_i) = \lim_{\Delta\theta_i \rightarrow 0} \frac{Q_i(\theta_i + (\Delta\theta_i/2)) - Q_i(\theta_i - (\Delta\theta_i/2))}{\Delta\theta_i}, \quad (23)$$

So by implementing the above equation on Eq. (22):

$$Q'_i(\theta_i) = \pi h^2 K \left[\frac{\tan^2((\theta_i/2) + (\Delta\theta_i/4)) - \tan^2((\theta_i/2) - (\Delta\theta_i/4))}{(\Delta\theta_i/2)} \right] \quad (24)$$

Then, by dividing Eq. (24) with (22):

$$Q'_i(\theta_i) = Q_i(\theta_i) \frac{\tan^2((\theta_i + (\Delta\theta_i/2))/2) - \tan^2((\theta_i - (\Delta\theta_i/2))/2)}{\tan^2(\theta_i/2)} \times \frac{2}{\Delta\theta_i} \quad (25)$$

Also

$$Q_i(\Delta\theta_i) = \frac{Q'_i(\theta_i) \times \Delta\theta_i}{2} \tag{26}$$

And evidently

$$\frac{Q_i}{Q_t} = \frac{\tan^2(\theta_i/2)}{\tan^2(\theta_{\max}/2)} \tag{27}$$

So according to Eqs. (25)–(27):

$$Q_i(\Delta\theta_i) = Q_t \frac{\tan^2((\theta_i + (\Delta\theta_i/2))/2) - \tan^2((\theta_i - (\Delta\theta_i/2))/2)}{\tan^2(\theta_{\max}/2)} \tag{28}$$

Q_t is the total flow rate from the nozzle. So any increments of the flow which have been discharged from a nozzle have been identified.

It is necessary to indicate that Eq. (28) is an absolute mathematical equation. It can be corrected by multiplication of an experimental parameter (f):

$$Q_i(\Delta\theta_i) = fQ_t \frac{\tan^2((\theta_i + (\Delta\theta_i/2))/2) - \tan^2((\theta_i - (\Delta\theta_i/2))/2)}{\tan^2(\theta_{\max}/2)} \tag{29}$$

In absence of experimental data, f can be regarded to be equal to 1 (ideal case).

10. Numerical solution

First of all and before solving Eq. (2) and the consequent calculating of the particle concentration distribution, the droplets size distribution should be derived. Energy balance has been used to determine the two variables, δ_G and D_G in Eq. (13), as follows.

Initially, two values for δ_G and D_G are speculated, and subsequently a droplet size i will be chosen. Then according to the cone model, a θ increment and an α increment are selected. Consequently a cone element is then specified (Eq. (29)). Then momentum equations (Eqs. (6)–(10)) are applied simultaneously with the PSI-CELL model (Eqs. (11) and (12)) to evaluate the droplet equivalent, z direction velocity, and also droplets volume and number flow rate. Also the momentum equations assess whether the selected cone increment has impacted the wall or not. If impacted, that increment will be stopped and transformed into the liquid film. These steps continue to further θ and α cone increments and further droplets sizes till all cone increments and droplets sizes are covered. Consequently at the end, the equivalent and z direction velocity as well as droplets number flow rate of each droplet size at any increment of the tower have been calculated. These variables are inserted in Eqs. (14)–(17) to obtain the gas temperature profile. If the calculated temperature profile is consistent with data, certainly the droplet size distribution in the tower has been obtained, else the sequences will go on to other δ_G and D_G .

After obtaining the droplet size distribution in the tower, the velocity and number flow rates of the droplets are inserted in Eq. (2) to obtain the concentration distribution profiles of the

particles. All of the equations have been solved by implicit Euler method. Also a MATLAB code has been written to solve and do the indicated sequences.

11. Results and discussion

By $\delta_G = 5$ and $D_G = 500 \mu\text{m}$, the temperature data and temperature profile obtained from Eqs. (14)–(17) do have the best coherence (Fig. 3). Fig. 4 shows the equivalent droplet size distribution. Fig. 5 demonstrates a comparison between the predicted

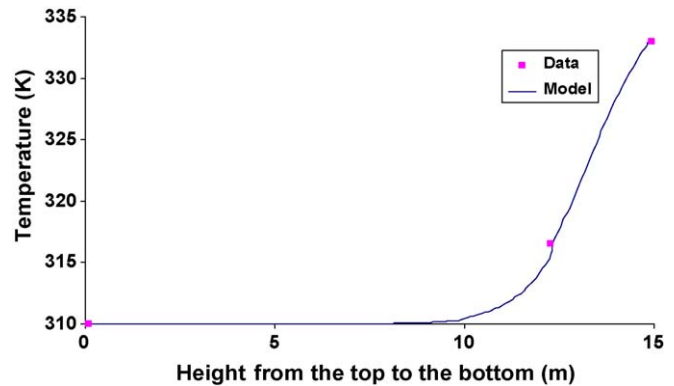


Fig. 3. Comparison of the temperature profiles obtained by $\delta_G = 5$ and $D_G = 500 \mu\text{m}$ with data.

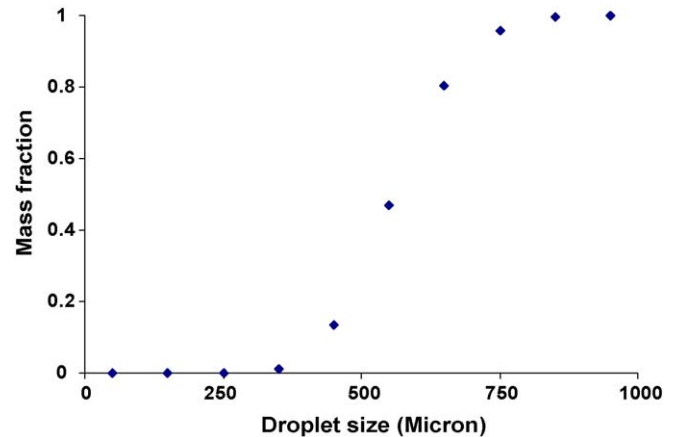


Fig. 4. Equivalent droplet size distribution in the studied scrubber.

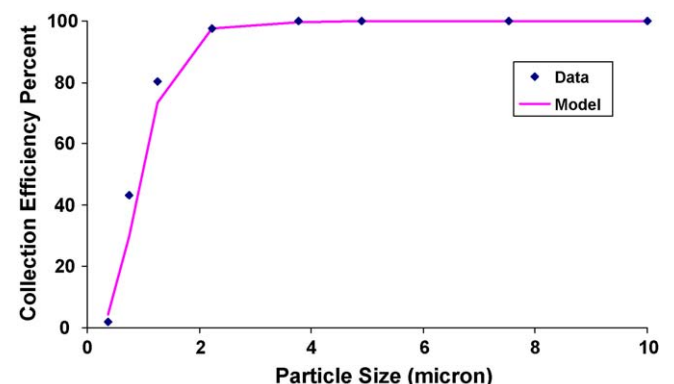


Fig. 5. Collection efficiency percent for data and the model.

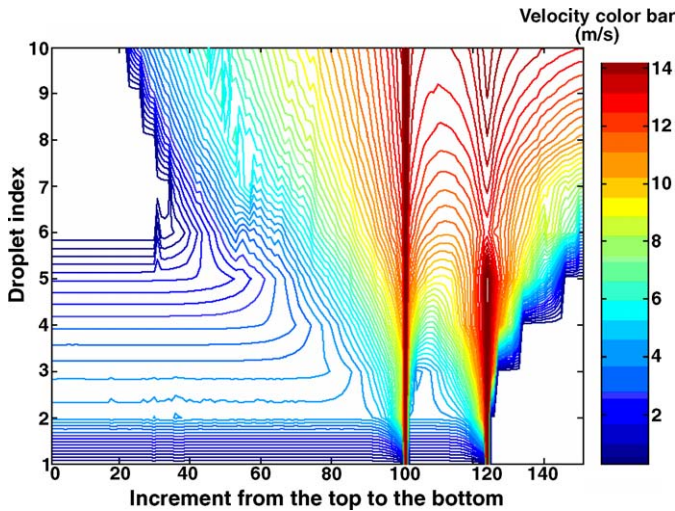


Fig. 6. Velocity profile of droplets at any increment of the tower with two rows of nozzles.

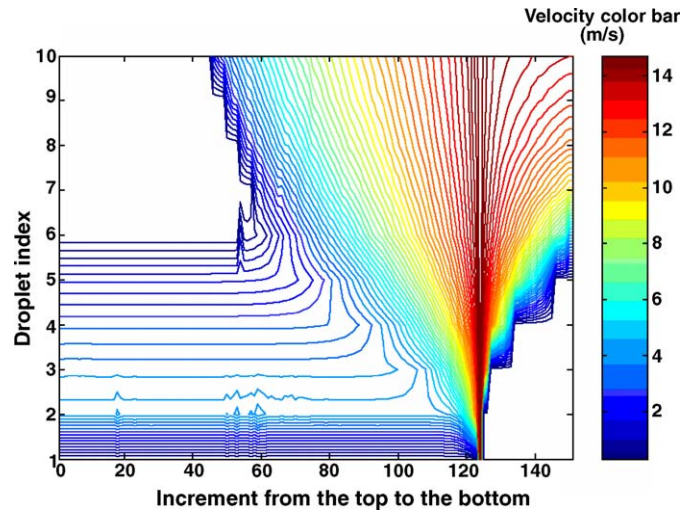


Fig. 7. Velocity profile of droplets at any increment of the tower with one row of nozzles.

collection efficiency percents for each particle cut size with the experimental data. As is evident, a good consistency has been observed between the data and the model.

After confirming the mathematical model, various parameters such as droplets velocity profile, liquid film, total projected surface area of the droplets and sauter diameter of the droplets have been studied based on the assumption of a constant diameter (3.18 m) all over the tower.

Fig. 6 shows the velocity profile of each droplet cut size at any segment of the tower when two rows of nozzles are installed. The horizontal coordinate stands for the tower increments, which by multiplication by 0.099 shows the distance from the top and vertical coordinate stands for the particle size index (Table 3). The color bar represents the velocity in m/s. In increments 101 and 124 or 10 and 12.2 m from the top, respectively, nozzle rows have been installed.

From Fig. 6, for descending droplets (from increment more than 101), the following results can be concluded:

- The smaller droplets would convert into the liquid film in higher sections of the tower.
- The larger droplets have larger velocities in lower sections in comparison with the smaller ones.
- Larger droplets velocities do not change much in contrast with the smaller ones.
- Nozzle zones possess the maximum velocity front.

For ascending droplets, the smaller the droplets are, the more they rise. But as is evident, their velocity is about the gas velocity. Also the velocity front in the higher row is greater than the lower one which brings about a higher mass transfer coefficient in this section. Fig. 7 shows the droplets velocity profile when one row of nozzles is installed.

Figs. 6 and 7 prove that increasing the number of nozzles rows can be beneficial in particle removing because it increases the droplets velocity in the spray tower. Also confirm the high amount of errors resulting from the assumption of a steady state

motion of the droplets with terminal velocity, especially for the smaller ones.

Fig. 8 shows the cumulative percentage of liquid film per total flow discharged from the nozzles (420 m³/h) at any height of the tower. It is evident that about 75% of the flow is transformed into liquid film in the studied scrubber.

One of the important observations in the liquid film formation simulation was with low velocity of droplets at the moment of impinging upon the spray tower wall. As a result, it has been observed that descending droplets, as moving counter currently with gas, are more subjected to converting into liquid film rather than ascending droplets. It has been observed that this effect escalates when the gas velocity increases. This is equivalent to more liquid film formation below the nozzles rather than the same corresponding height above the nozzles. So the flow of droplets in the upper row of nozzles is more than the other one.

Fig. 9 demonstrates the error when liquid film has been ignored in the studied scrubber. In other words, v_r and v_θ have been eliminated from the momentum equations for the droplets. By taking Fig. 9 into account, it is proven that for the particles smaller than 1 μm , the error percent is more than for the larger ones; but generally, as is evident, liquid film formation

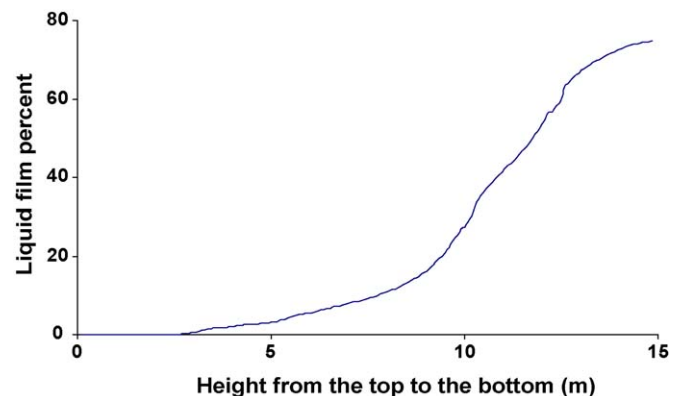


Fig. 8. Percentage of liquid film per total liquid discharged from nozzles.

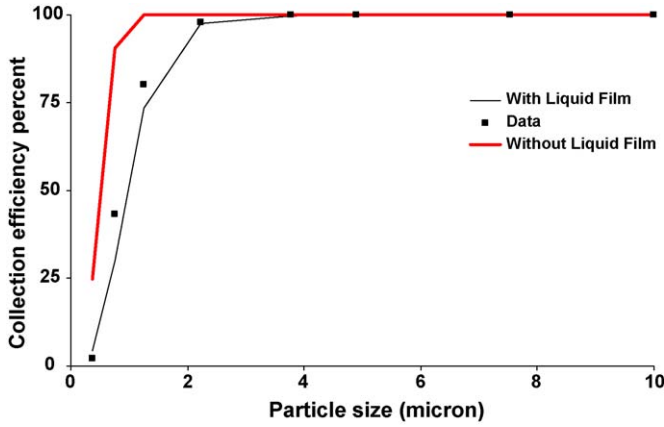


Fig. 9. Comparison of the collection efficiency percents for each particle cut size predicted by the models with data.

has no significant effect in the particle removing process. This is attributed to the low velocity of the droplets at the moment of impinging on the wall. Hence, according to Eq. (2), this phenomenon reduces the driving force for removing of the particles.

In particulate scrubbing, unlike gas scrubbing, this is the projected surface area of the droplets which is engaged in the cleaning process. This quantity is obtained by:

Total projected surface area of the droplets at any increment of the tower =
$$\sum_{D_{i\min}}^{D_{i\max}} \frac{Q(i, z)}{(\pi D_i^3/6)} \times \left(\frac{\pi D_i^2}{4} \right) \frac{dz}{v_z(i, z)} \quad (30)$$

And also

Total projected surface area of the droplets per unit time at any increment of the tower =
$$\sum_{D_{i\min}}^{D_{i\max}} \frac{Q(i, z)}{(\pi D_i^3/6)} \times \frac{\pi D_i^2}{4} \quad (31)$$

The current quantities are involved in the particle removing equation (Eq. (2)) directly. Fig. 10 shows the total projected surface area of the droplets per unit time at any height of the tower from the top to the bottom. The peaks are the nozzle locations. It is noticeable that the maximum is on the higher row of nozzles, not the lower one. This is attributed to the higher amount of flow

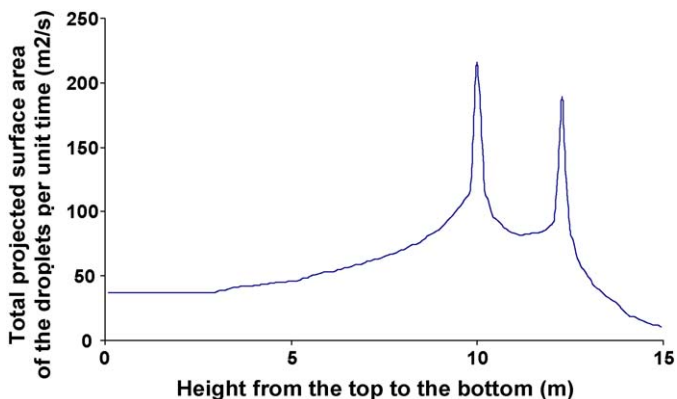


Fig. 10. Total projected surface area of the droplets per unit of time.

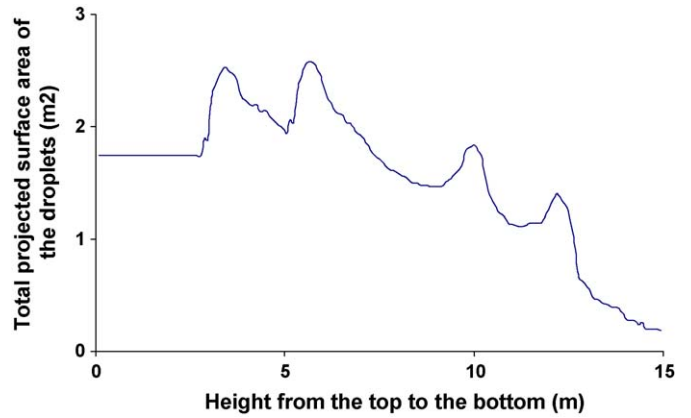


Fig. 11. Total projected surface area of the droplets.

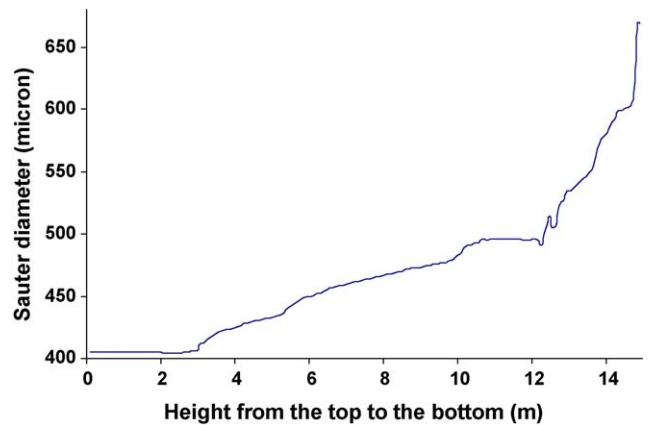


Fig. 12. Sauter diameter vs. tower height at any section of the tower.

in the higher one in comparison with the lower one which has been discussed before.

Fig. 11 shows the total projected surface area of the droplets at any section of the tower. The unusual form of this figure is attributed to the effect of velocity in Eq. (30). As can be seen, the z direction velocity influences this quantity other than the flow in each increment.

Sauter diameter evolution (because of liquid film) versus the tower length are shown in Figs. 12 and 13. As it is evident,

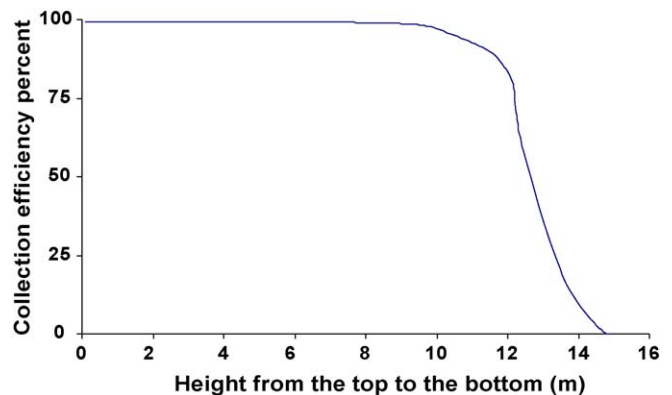


Fig. 13. Collection efficiency percent vs. the height for particles of 1.52–2.95 μm .

while the droplets are going down, the sauter diameter increases, unlike what happens while going up. This evidence proves that for droplets going downward, the smaller the droplets are, the sooner they convert into liquid film. The reverse is true for droplets moving upward. But it has been observed that when the diameter of the tower increases, the sauter diameter of the droplets in each increment of the tower do not change significantly. Therefore it seems that the liquid film contribution in droplet size evolution is ignorable in big spray scrubbers. This is consistent with Makkinejad's [6] results. But according to her, this result is not consistent for her small pilot plant towers.

According to Azzopardi and coworkers [14], one of the major problems in venturi scrubbers is the evolution of the droplet size distribution in the throat. It means that the droplet size distribution along the throat is something different than that of droplet size at the point of water injection. According to them, and as far as we aware, up to now, there is no mathematical model to explain the droplet size change along a venturi scrubber or any kind of scrubber. So the droplet size distribution at the nozzles points cannot confidently be used as the real droplet size distribution in the scrubber length. This phenomenon, in the scrubbers, can be attributed to the evaporation, droplet coagulation or disintegration, turbulence (in venturi [16] or orifice types) and also liquid film formation. According to Azzopardi et al., droplets diameter evolution due to evaporation is ignorable in their venturi pilot plant scrubber which logically can be generalized to spray types with low or moderate gas temperatures. As a whole, droplet size evolution in spray scrubbers can be attributed to the liquid film formation and droplets coagulation or disintegration. But it seems that further studies should be made on the contribution of droplets coagulation or disintegration.

In a gaseous pollutant scrubbing process, the maximum mass transfer operation zones are located in the nozzles locations [5,8]. But Fig. 13, as is typical for the particle size from 1.52 to 2.59 μm , shows that this hypothesis is not consistent for the particle removing process. This phenomenon has been observed for the other particle sizes, especially the larger ones.

12. Conclusions

The droplets dynamic behavior is simulated by the Lagrangian approach based on PSI-CELL model. Also, a particles removal process has been modeled in Eulerian frame. Many variables effects on the performance of the spray scrubber have been discussed.

It has been observed that liquid film formation has no significant effect on the particle removing process and the smaller droplets have a greater contribution in liquid film formation. In addition, the assumption of terminal velocity for the motion of droplets, especially for the smaller ones is a rough assumption.

It has been discussed that in big spray scrubbers, the droplets size evolution can be attributed to the coagulation and not liquid film formation. But the extent of the role of droplets coagulation or disintegration needs more research and experimental data.

References

- [1] R. Pigford, C. Pyle, Performance characteristics of spray type absorption equipment, *Ind. Eng. Chem.* 43 (1951) 1649–1662.
- [2] M. Sharma, K. Mehta, Mass transfer in spray towers, *Br. Chem. Eng.* 15 (1970) 1440–1444.
- [3] K.G.T. Hollands, An analysis of a counterflow spray cooling tower, *Int. J. Heat Mass Transf.* 17 (1974) 1227.
- [4] J. Michalski, Aerodynamic characteristics of FGD spray towers, *Chem. Eng. Technol.* 20 (1997) 108–117.
- [5] C. Brogen, H. Karlsson, Modeling the absorption of SO_2 in a spray scrubber using the penetration theory, *Chem. Eng. Sci.* 52 (1997) 3085–3099.
- [6] N. Makkinejad, Temperature profile in countercurrent/cocurrent spray towers, *Int. J. Heat Mass Transf.* 44 (2001) 429–442.
- [7] A. Rahimi, M. Taheri, J. Fathikaljahi, Mathematical modeling of heat and mass transfer in hot gas spray systems, *Chem. Eng. Commun.* 189 (2002) 959–973.
- [8] M. Meyer, M. Hendou, M. Prevost, Simultaneous heat and mass transfer model for spray tower design: application on VOCs removal, *Comput. Chem. Eng.* 18 (1995) 434–439.
- [9] M. Crawford, *Air Pollution Control Theory*, McGraw-Hill Book Company, New York, 1976.
- [10] K. Masters, *Spray Drying: An Introduction to Principles, Operational Particle and Applications*, John Wiley & Sons, New York, 1976.
- [11] S. Calvert, Venturi and other atomizing scrubbers efficiency and pressure drop, *AIChE J.* 16 (1970) 392–396.
- [12] M. Mohebbi, M. Taheri, J. Fathikaljahi, M.R. Talaie, Simulation of an orifice scrubber performance based on Eulerian/Lagrangian method, *J. Hazard. Mater. A100* (2003) 13–25.
- [13] A. Mohebbi, M. Taheri, J. Fathikaljahi, M.R. Talaie, Prediction of pressure drop in an orifice based on Lagrangian approach, *J. Air Waste Manag. Assoc.* 52 (2002) 174–178.
- [14] D.F. Alenso, J.A.S. Goncalves, B.J. Azzopardi, J.R. Coury, Drop size measurement in venturi scrubbers, *Chem. Eng. Sci.* 56 (2001) 4901–4911.
- [15] C. Crowe, M. Sharma, D. Stock, The particle-source-in Cell (PSI-CELL) model for gas-droplet flows, *ASME J. Fluids Eng.* (1977) 325.
- [16] P. Bayvel, Application of the laser beam scattering technique method for multi phase flow investigation, in: *Proceedings of the Conference on Multiphase Transport, Fundamentals and Reactor Safety Applications*, Hemisphere Book Company, New York, 1980.